International Journal of Computer Information Systems and Industrial Management Applications
ISSN 2150-7988 Volume 18(14s) 2026 pp. 520-538
https://doi.org/10.70917/ijcisim-2026-3357
Article

Diagnosis of Alzheimer's Disease and Frontotemporal Dementia from Electroencephalography Signals

P. Gopala Krishna[1,*] , J. Somasekar[2]

[1,*] Department of Computer Science and Engineering, Faculty of Engineering and Technology, JAIN (Deemed-to-be University), Bangalore 562112, Karnataka, India
[2] Department of Computer Science and Engineering, Faculty of Engineering and Technology, JAIN (Deemed-to-be University), Bangalore 562112, Karnataka, India.
Email: gopalak.cse@gmail.com[1, *], somasekar.j@jainuniversity.ac.in [2]

Abstract: Alzheimer's Disease (AD) and Frontotemporal Dementia (FTD) are progressive neurodegenerative disorders that impair cognition, behaviour, and daily functioning, creating significant challenges for early and accurate diagnosis. Their overlapping clinical symptoms make difficult to distinguish AD, FTD, and Cognitively Normal (CN) individuals during the early stages, delaying appropriate intervention and treatment planning. Existing diagnostic approaches are limited by their reliance on binary classification, lack of direct feature extraction for AD–FTD discrimination, and insufficient capability to identify nonlinear irregularities and frequency redistribution patterns in electroencephalography (EEG) signals. To overcome these limitations, this study proposes a novel EEG-based multiclass classification framework using comprehensive multi-domain feature analysis. EEG signals are preprocessed through filtering, artifact removal, re-referencing, and segmentation to improve signal quality. Discriminative features are extracted from time-domain, frequency-domain, and time-frequency complexity measures, providing a comprehensive representation of neural activity. Classification is performed using nonlinear Support Vector Machine (SVM) model to distinguish AD, FTD, and CN groups effectively. Experimental results demonstrate high classification accuracy, strong class separability, and robust predictive performance with minimal misclassification. The findings confirm that the proposed integrated framework provides a reliable, efficient, and clinically valuable approach for early dementia detection, accurate differential diagnosis, and improved decision-making in clinical practice.

Keywords: Alzheimer's disease, Electroencephalography, Frontotemporal Dementia, Support Vector Machine.

1. Introduction

Frontotemporal Dementia (FTD) is a neurodegenerative disorder primarily affecting the frontal and anterior temporal lobes of the brain [1]. It is typically seen occurring more in middle-aged adults, with an onset age ranging from 45 to 65 years [2,3]. Because of the specific areas of degeneration, FTD is associated with specific behavioural and language issues due to the loss of nerve cells in both areas [4-6]. Currently, there are no approved disease-modifying therapies for the treatment of FTD [7,8]. Pharmacological therapies that have been found effective in Alzheimer's disease do not significantly benefit FTD patients [9,10]. On the other hand, Alzheimer's disease (AD) is the most common type of dementia and usually affects memory and cognition, which progress over time. The AD & FTD have similarities in clinical presentation, but at the same time are different and is illustrated in Figure 1 [11,12]. Because of the overlap between the two dementia types, diagnosing the two types early and accurately is a large clinical hurdle [13]. Electroencephalography (EEG) has been viewed as a good tool to help aid in diagnosing FTD and Alzheimer's type dementias as it is a non-invasive test that can detect brain activity using scalp electrodes [14]. Recent advances in neurophysiological analysis and machine learning have introduced diverse EEG-based approaches for differentiating Alzheimer's disease (AD) and Frontotemporal Dementia (FTD). A graph-theoretic functional connectivity framework was proposed to analyse alterations in brain networks of AD and FTD patients, where

topological metrics such as clustering coefficient and path length were used to characterise disrupted neural communication patterns [15]. In addition, EEG-based neural biomarker modelling combined with predictive analytics has been explored for early diagnosis of mild cognitive impairment and AD, leveraging advanced signal processing and feature selection strategies [16]. Furthermore, quantitative EEG feature investigations revealed that conventional processed indices used in anaesthesia monitoring fail to adequately capture disease-specific EEG alterations in AD and FTD, emphasising the need for disorder-oriented feature extraction methods [17]. Deep learning (DL) techniques, particularly Convolutional Neural Networks (CNNs), have also been employed to automatically learn discriminative EEG representations for AD detection, incorporating segment length optimisation to enhance classification performance [18]. However, many of these approaches rely either on complex network modelling, highly data-driven deep architectures requiring large datasets, or indirect EEG indices that may not explicitly capture nonlinear irregularity and frequency redistribution characteristics.

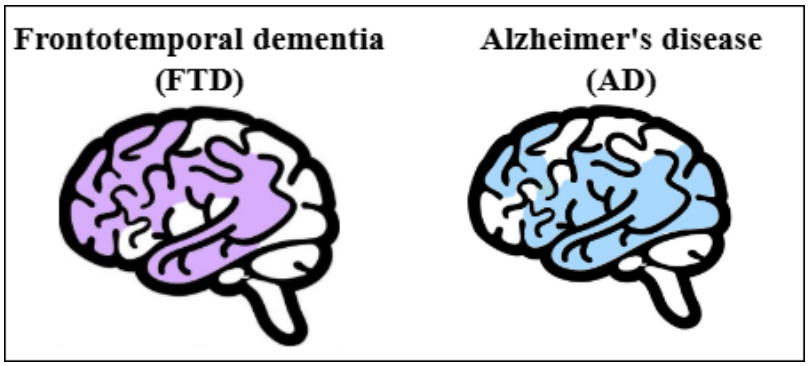

Figure 1: Visualization of Brain regions affected by FTD and AD. FTD primarily involves degeneration in the frontal and temporal lobes, which leads to behavioural and language impairments. In contrast, AD mainly affects the hippocampus and temporoparietal regions associated with memory and cognitive decline. The figure highlights the distinct patterns of brain atrophy that help differentiate the two disorders.

Therefore, a hybrid time frequency entropy-based EEG framework that integrates domain-specific handcrafted features with robust machine learning classification remains essential for achieving accurate and interpretable multi-class differentiation between AD, FTD, and normal subjects.

1.1 Research Contributions

The study makes the following key contributions to EEG-based diagnosis of Alzheimer's Disease (AD) and Frontotemporal Dementia (FTD):

- **Hybrid Multi-Domain EEG Feature Extraction:** The proposed EEG feature extraction framework that integrates time-domain, frequency-domain, and time-frequency-domain EEG features to collectively represent both linear and nonlinear neural dynamics related to dementia.
- **Entropy-Based EEG Complexity Analysis:** The proposed framework introduces the view of using spectral entropy as a measure of EEG irregularity and frequency shift in the EEG to enhance the capacity to detect subtle neurodegenerative changes in AD and FTD.
- **Improved Classification by Multi-Domain Integration:** By combining multiple domain features, the framework can overcome the limitations of single-domain-based methods to enable more robust classifications across datasets with imbalanced datasets and small sample sizes, thus providing overall improved diagnostic accuracy.
- **Robust Multi-Class Dementia Classification Model:** The proposed SVM with Radial Basis Function (RBF) kernel will provide a robust framework for the multi-class Alzheimer's Disease (AD), Frontotemporal Dementia (FTD), and Cognitively Normal (CN) classification of subjects, providing reliable differential diagnostic capabilities during early clinical screening

The manuscript is structured as follows Section 2 includes a review of literature regarding EEG-based methods for the diagnosis of dementia, Section 3 provides an overview of the time-frequency entropy framework developed for this study, Section 4 describes the findings from the study, and Section 5 summarizes the conclusions and provides future recommendations.

2. Related works

Analysing EEG-based diagnostic techniques of both FTD and AD. It will also situation methodologies in the following areas signal preprocessing methodologies, feature extraction methodologies, classification methodologies, and accurate multi-class dementia detection using for accurate multi-class dementia detection. Le et al. [19] developed an approach to individual AD, FTD, and CN using EEG time-domain analysis and achieve cost-effective approach for separating AD from FTD. However, the fixed window segmentation is validated across larger datasets and clinical trials to ensure generalizability and robustness in real-world diagnostic situations.

Akbar et al. [20] focused on Neuro Fusion Net, a hybrid DL framework using a one-dimensional convolutional neural network (1D-CNN) to create a clinically applicable solution for distinguishing AD from other dementias classification based on EEG data analysis. However, the multimodal integration, progression prediction, and portable real-time monitoring make Neuro Fusion Net clinically scalable and practical.

Ohal et al. [21] developed a comprehensive evaluation of the EEG signal and analysis techniques for the early diagnosis of AD through the application of ML algorithms. However, this integration, algorithm refinement, and longitudinal validation of identifying potential early symptoms of AD would enhance the remote diagnosis of Alzheimer's.

Abadal et al. [22] focused on GNNs for the EEG-based detection of AD and discrimination of two different types of seizures using an ML model demonstrate the value of GNNs by showing that a single GNN architecture. However, this investigation is scaling to larger EEG datasets, optimising inference with hardware accelerators, and validating across diverse clinical populations for broader applicability.

Si et al. [23] developed a constructed frequency-based multilayer resting-state EEG network and extracted representative network features to improve the differentiation between AD and FTD using machine learning (ML) algorithms, and GNB demonstrates higher classification than other classification algorithms. However, the cognitive tasks to conduct an in-depth analysis, to explore the mechanism underlying the variability between AD and FTD, Puri, D. V et al. [24] focused on AD using spatiotemporal EEG Analysis and a low-complexity CNN called LEADNet to generate disease-specific features achieve high accuracy while maintaining computational efficiency suitable for practical deployment. However, further validation on larger and multi-centre datasets is required to confirm its generalizability. By analysing the existing models, EEG-based dementia diagnosis models have significant challenges in accurately distinguishing AD, FTD and CN as a result of overlapping cognitive decline, shared neural characteristics and variability/difficulty in EEG recordings. Many existing approaches rely on single-domain features, or use a DL approach that requires very large data sizes, thus hindering generalizability, interpretability and clinical scalability. Furthermore, several methods fail to capture nonlinear irregularity, frequency redistribution, and integrated multi-domain neural dynamics that can be used for a true differential diagnosis. Hence, there is a critical demand for a computationally efficient and clinically interpretable EEG framework that can effectively integrate complementary signal characteristics while accommodating small sample sizes and addressing issues of class imbalance. Accordingly, we propose the use of a hybrid time-frequency-entropy-based EEG framework that combines Hjorth parameters, band power, spectral entropy and wavelet entropy with nonlinear SVM-based multi-class classification to obtain improved diagnostic accuracy and reliable early detection of dementia.

3. Proposed Methodology

The proposed framework presents a hybrid time frequency entropy-based EEG method for the multi-class diagnosis of Alzheimer's Disease (AD), Frontotemporal Dementia (FTD), and Cognitively Normal (CN) subjects. EEG signals are obtained from the OpenNeuro dataset [25], and preprocessed using bandpass filtering of the data to isolate neural frequencies and performed Notch filtering of the signals to eliminate power line interference. After processing, signals were segmented into fixed-length 80-second temporal windows to facilitate consistent temporal representation and temporal stability of feature extraction. A two-part feature extraction method is implemented. Time domain features were derived from Hjorth parameters that resolve the variance and temporal dynamics of the signals. Frequency domain features consider the band powers of the signal and spectral entropy values of the signal, to describe the frequency redistributions of power and non-linear neural irregularities associated with dementia. Time and frequency domain features include wavelet entropy from the time frequency analysis to represent localized nonlinear complexity. Each normalized feature set is standardized using Z scores and combined as a single feature set. Finally, a Support Vector Machine (SVM) using a Radial Basis Function (RBF) kernel is used to obtain reliable multi-class classifications to allow for accurate differential diagnoses and potentially improved early diagnosis of dementia as shown in Figure 2.

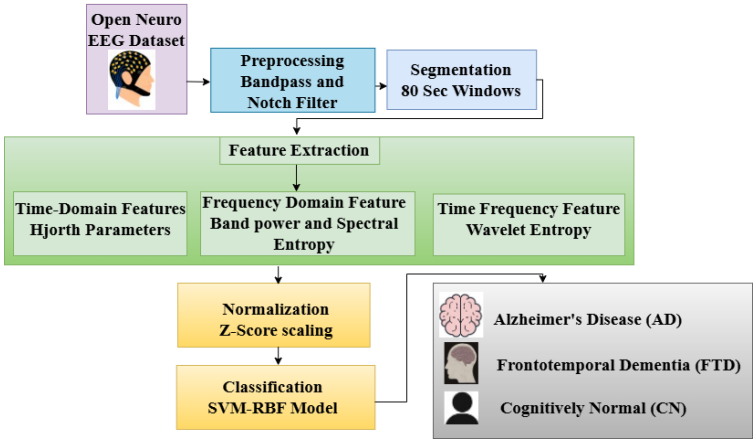

Figure 2: Schematic representation of the proposed framework for Alzheimer's Disease and Frontotemporal Dementia classification

3.1 Dataset

The Open Neuro dataset provides the EEG data for 88 subjects, where 36 diagnosed with AD, 23 diagnosed with FTD, and 29 with CN. Cognitive evaluation was conducted by the Mini-Mental State Exam (MMSE). Average scores on the MMSE were 17.75 for AD, 22.17 for FTD, and 30 for CN. The average age in years of those with AD was 66.4 while that of those with FTD was 63.6 and CN was 67.9. EEG data was collected using the Nihon Kohden EEG 2100 using 19 scalp electrodes and 2 reference electrodes positioned on the mastoids, according to the 10-20 system. The raw data was sampled at a rate of 500 Hz with loads of less than 5 kΩ and was recorded over approximately 12-13.8 minutes per participant. The EEG signals were then pre-processed. Eye and jaw-related artefacts were eliminated from the EEG using artefact subspace reconstruction (ASR) and independent component analysis (ICA).

3.1.1 Preprocessing of EEG Signals

All completed EEG signals were compared with the Open Neuro database to check for standardisation [26]. The time series were resampled at a sample rate of 128 Hz, providing all data with the same temporal resolution. A Finite Impulse Response (FIR) [27] band-pass filter (0.5-45 Hz) was then used on processed data to keep the relevant physiological EEG frequency range and eliminate low-frequency drifts and high-frequency noise. Finally, A 50 Hz notch filter was included in the processing of each EEG to eliminate control line noise. The Common Average Reference (CAR) method was then used on processed data. These processes resulted in producing clean, noise-free, standardised EEG data that were ready for multi-domain feature extraction and classification.

3.2 Segmentation of the EEG signals

Segmenting EEG data is a significant step in the treatment of signals, which helps in systematic analysis of data and to obtain meaningful features through the division of a continuous recording into multiple smaller segments. After pre-processing, the EEG signals were filtered and then segmented into fixed-length segments to maximize the data usage and to improve classification robustness, especially for small sample sizes. In this study, the proposed methodology defined that the signals would be segmented into non-overlapping 80-second windows. Each segment was treated as an independent sample while retaining original class labels (AD, FTD, and Normal). This segmentation strategy increased the real number of training samples without altering the class distribution, thereby supporting stable feature extraction and improving the performance of the multiclass SVM classifier.

3.3 Feature Analysis

The EEG features Analysis discriminative capability for differentiating AD, FTD, and CN subjects using time-domain (Hjorth), frequency-domain (band power and spectral entropy), and time-frequency (wavelet entropy) features to understand signal variance, frequency redistribution, and nonlinear complexity. The combined feature set makes class separation better and increases the strength of multi-class dementia classification.

3.3.1 Hjorth parameters

Hjorth parameters represent statistical measures employed in time-domain signal analysis. Hjorth first presented them in 1970. These parameters consist of three key metrics: activity, mobility, and complexity. They are commonly used in the analysis of EEG signals for feature extraction and are referred to as normalised slope descriptors (NSDs). Alongside EEG analysis, they are utilised in examining EEG signals [28].

Activity

This parameter indicates the power of the signal, which is defined as the variance of a time-dependent function. It measures the energy or dispersion of the signal around the average and relates to the area under the power spectrum within the frequency range as shown in Equation (1).

$$Activity = var(y(t)) \tag{1}$$

Where $var(y(t))$ denotes the variance of the signal $y(t)$.

Mobility

Mobility indicates the average rate or standard deviation of the power spectrum. It is determined by taking the square root of the ratio between the variance of the signal's first derived and the variance of the signal itself, as demonstrated in Equation (2).

$$Mobility = \sqrt{\frac{var\left(\frac{dy(t)}{dt}\right)}{var(y(t))}} \tag{2}$$

Here, $\frac{dy(t)}{dt}$ is the first derivative of the signal $y(t)$, providing a measure of the signal's rate of change.

Complexity

This is a metric for identifying the variation in Mobility. The change in frequency is evaluated to determine how much the signal looks like a pure sine wave, with values nearing 1 signifying a higher similarity. It is computed using the mobility of the initial and secondary derivatives of the signal as in Equation (3).

$$Complexity = \frac{Mobility\left(\frac{d^2y(t)}{dt^2}\right)}{Mobility\left(\frac{dy(t)}{dt}\right)} \tag{3}$$

Where $\frac{d^2y(t)}{dt^2}$ is the second derivative of y (t). This parameter captures the signal's intricacy by assessing frequency variations. In this study, we computed the local Hjorth parameters across the complete seismic cube utilising the Python programming language.

We utilised the resulting cube from each parameter as a seismic attribute along with the chosen attributes. We employed a window size of 18 to determine each local feature. Employing a broader window for computations led to smudged geological details, whereas utilising a narrower window causes information loss and produces undefined values.

3.3.2 Frequency Domain Features (Band power, Spectral Entropy)

EEG frequency-domain analysis plays a critical role in identifying neurophysiological alterations associated with AD and FTD [29]. Prior studies, including diagnosis of AD and FTD from EEG signals, have reported that dementia is characterised by spectral slowing, defined as a redistribution of oscillatory energy toward lower frequency bands.

Band power

Power Spectral Density (PSD) is computed using Welch's method [30] after preprocessing. The EEG signal is decomposed into standard frequency bands. Delta (0.5–4 Hz), Theta (4–8 Hz), Alpha (8–13 Hz), Beta (13–30 Hz) for each of the 19 EEG channels is defined using Equation (4).

$$BP_{b,c} = \int_{h_1}^{h_2} PSD(f)\, df \tag{4}$$

Where BP Band power of the band b in channel c, h_2, h_1 are lower and upper frequency limits of the band, $PSD(f)$ is the power spectral density of the channel c, and f is the frequency variable.

Power reflects the redistribution of oscillatory energy, which is associated with dementia. This phenomenon is referred to as EEG slowing, a well-documented biomarker in AD and FTD. The shift from higher-frequency fluctuations alpha and beta toward slower rhythms delta and theta reflects impaired synaptic transmission, cortical disconnection, and neuronal degeneration. For 4 bands × 19 channels features.

Spectral Entropy

Spectral Entropy (SE) is used to measure the randomness and complexity of the normalised power spectrum [31]. Spectral entropy is based on Shannon entropy and indicates how uniformly the power of a signal is spread out over different frequency bins in equation (5)

$$R_c = -\sum p(h) \log P(h) \quad (5)$$

where R_c is the Spectral entropy of the channel c, $p(h)$ is the normalised power at the frequency bin c , and h is the frequency bins. Higher values of spectral entropy indicate a more uniform distribution of power among various frequency components, which means that the neural activity is complex and flexible.

The lower values of spectral entropy mean that there is an uneven distribution of power, usually dominated by low-frequency components, indicating less complexity in the signal and less adaptability in the neural system. There are $1 \times 19 = 19$ features of spectral entropy and the measures of entropy per electrode thus improving spatial sensitivity by allowing for localized reductions of complexity within different regions of the cortex.

3.3.3 Time frequency Feature (Wavelet Entropy)

Wavelet Entropy (WE) acts as a feature in the time-frequency domain for measuring complexity and irregularity in non-stationary EEG signals [32]. The wavelet transforms, which allow multi-resolution decomposition, provide simultaneous localization in time and frequency domains and thus more effective than traditional spectral analysis. This characteristic makes it very apt for observing slight changes in neural dynamics related to AD and FTD.

Wavelet Entropy is applied here to describe how the energy of the signal is distributed over different wavelet sub-bands, which gives an idea about the complexity of EEG signals within a time-frequency framework. It does not play a role as a parameter selection criterion in this framework as derived in Equation (6).

$$H_j^i = \frac{|r^i(i)|}{\sum_{j=1}^{M^i} |r^i(j)|} \quad (6)$$

Where i is the index of the wavelet sub-band, j is the index of the wavelet coefficient within the $i-th$ sub-band, j is the Wavelet coefficient at the position j in sub-band i, $r^i(i)$ is the absolute value of the wavelet coefficient, M^i is the total number of wavelet coefficients in the $i-th$ sub-band, H_j^i is the normalized distribution of wavelet coefficients within each sub-band i. The wavelet entropy R^i is calculated by Equation (7)

$$R^i = -\sum_{i=1}^{M^i} H_j^i \log H_j^i \quad (7)$$

Where R^i is the Wavelet entropy of $i-th$ the sub-band, and $l$og the logarithmic function. Wavelet entropy measures the degree of disorder in the energy distribution across wavelet coefficients. When entropy values are high, it means that the energy is more evenly spread out across the time-frequency components. This situation typically signifies a higher level of complexity in the signal and greater variability in the neurons. Lower entropy values indicate energy concentration in fewer coefficients, suggesting reduced complexity and increased rhythmic dominance.

In dementia conditions such as AD and FTD, neural degeneration and cortical disconnection lead to reduced dynamical complexity, which is reflected as decreased wavelet entropy. In this framework, Wavelet entropy is used solely as a complexity feature and does not serve as a wavelet parameter selection criterion. Since it is computed independently for each of the 19 EEG channels, $1 \times 19 = 19$ wavelet entropy features. These channel-wise features enhance spatial sensitivity and enable the detection of localized complexity reductions across cortical regions.

3.4 Normalization through Z-score

The feature normalization is performed using Z-score normalization [33]. The proposed framework integrates multi-domain features and different numerical ranges and units. If the data is not normalized, the larger-magnitude features could dominate the classification learning process. This transforms each feature into a distribution with zero mean and unit variance. For any feature x, we can calculate its normalized value Z as follows in Equation (8)

$$Q = \frac{y-\beta}{\rho} \tag{8}$$

Where y is the original feature value, $\beta\ is\ the$ average feature value calculated across the training dataset, ρ is the Standard deviation of the feature computed across the training dataset. and Q is the normalized feature value. By normalizing, the average value for each of the features becomes 0, and the standard deviation of the features becomes 1. Normalizing ensures that all feature scales are balanced, increases numerical stability, and increases the performance of the SVM-RBF [34] kernel classifier by eliminating feature dominance due to scaling differences.

3.5 SVM with RBF

In classifying normal AD and FTD using EEG features, an SVM using a circular basis function RBF kernel has been determined appropriate, given its ability to effectively handle the nonlinear feature space frequently produced with multi-domain EEG features [35]. The RBF kernel project inputs features into a higher-dimensional space to allow for appropriate separation of more complex class boundaries. This makes it useful for use when performing classification tasks that require the separation of nonlinear patterns described in the original EEG data.

The RBF kernel is defined as Equation (9)

$$S(y_i, x_j) = exp(-\delta||y_i, x_j||^2) \tag{9}$$

$S(y_i, x_j)$ is the RBF kernel function value between feature vectors y_i and x_j , δ is the Kernel hyperparameter that controls the influence of individual data points, $||y_i, x_j||^2$ is the Squared Euclidean distance between the two feature vectors.

The SVM with RBF has two primary hyperparameters, the regularisation parameter C and gamma (γ). The C hyperparameter identifies a trade-off between increasing the margin of an SVM and decreasing the misclassification of samples during training. As C gets larger, it forces the classifier to refine errors more strictly, potentially reducing bias but increasing the risk of overfitting. The second hyperparameter is δ, which determines the influence of a single training example reaches. Higher values create a narrower influence, leading to increasingly complex classification surfaces. Lower values increase this radius of influence and results in smoother decision boundaries. The recent EEG-based dementia classification studies have shown that SVM with RBF effectively captures nonlinear relationships among complex EEG features, making it a robust choice for multi-class classification in AD and FTD detection.

4. Results and Discussion

In this section, we describe the experimental configuration and parameter settings used for the proposed EEG-based neurodegenerative disease classification framework. The dataset used for the implementation includes three classes of labeled samples AD Label A = 0, FTD, Label F = 1, and CN individuals Label C = 2) and consisted of EEG data collected as 80-second segments with a sample rate of 500 Hz. The EEG data was processed using an 0.5 - 45 Hz band pass filter and a notch filter at 50 Hz to remove noise and eliminate the power line interference during the preprocessing phase. This analysis was shown on the frequency range of normal EEG bands Delta (0.5 - 4 Hz), Theta (4 - 8 Hz), Alpha (8 - 13 Hz), Beta (13 - 30 Hz), and Gamma (30 - 45 Hz). The dataset was randomly separated into three sets 70% training, 10% validation, and 20% testing. Feature normalization was performed using the StandardScaler class to normalize the training set, thus preventing data leakage. The SVC model with the Radial Basis Function (RBF) kernel was qualified to generate a classification of the dataset, using C = 100 and Gamma = 0.01 to optimize the separation of decision boundaries are described in Table 1.

Table 1: Parameters involved in the Proposed Model and Value Settings

Section	Parameter	Value
	Label A	0

Dataset	Label F	1
	Label C	2
Signal Acquisition	Segment Length	80 seconds
	Sampling Frequency (FS)	500 Hz
Preprocessing	Bandpass Filter	0.5 – 45 Hz
	Notch Filter	50 Hz
Frequency Bands	Delta	0.5 – 4 Hz
	Theta	4 – 8 Hz
	Alpha	8 – 13 Hz
	Beta	13 – 30 Hz
	Gamma	30 – 45 Hz
Data Splitting	Training Set	70%
	Validation Set	10%
	Test Set	20%
Normalization	Method	StandardScaler
	Fitted On	Training Set Only
Classifier	Model	Support Vector Machine (SVC)
	Kernel	RBF
	C	100
	Gamma	0.01

4.1 Performance Evaluation of the Proposed Framework

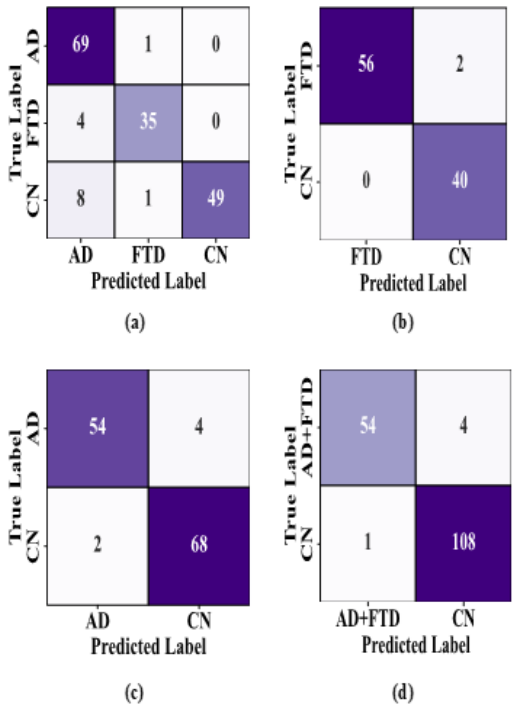

Figure 3: Confusion Matrix Analysis for Dementia Classification

This section evaluates the proposed EEG-based classification framework using various performance metrics to judge how reliably it can differentiate AD, FTD, and CN. The results show strong multi-class diagnostic capability through the use of time-domain, frequency-domain, and entropy features with an SVM classifier.

The overall accuracy of 92.1%, indicates that the model has high accuracy when classifying individuals according to each of the three diagnostic groups. The precision (91.7%) and recall (92.4%) for the detection of accurate dementia cases, as well as the F1-score (91.9%), verify that the model detects almost all dementia cases correctly while at the same time producing very few false-positive classifications. This analysis demonstrated high specificity (91.6%) and NPV (92.3%). The results of the MCC value (87.2%) provide evidence of the robustness of the proposed framework. Furthermore, the low false-positive rate (FPR) of 0.082 and the false-negative rate (FNR) of 0.074 support the conclusion that there are very few misclassifications. Finally, the AUC of 95.6% indicates that the proposed model has an excellent ability to distinguish between different diagnoses.

Figure 3 shows the confusion matrices for different classification scenarios. The three classifications are represented in Figure 3(a) by comparing the three diagnoses of AD, FTD, and CN. The model identifies the majority of the subjects within each of the three classifications: AD (69), FTD (35), and CN (49). A small number of CN cases are misclassified as AD, and a few FTD cases are predicted as AD, indicating slight overlap between these classes. Figure 3(b) shows total FTD cases (56) and CN cases (40) were classified as expected by the model. However, 2 of the FTD cases were misclassified as CN. The model demonstrates clear discrimination between the FTD subjects and the cognitively normal subjects. Figure 3(c) shows the binary classification of AD versus CN cases. In the total of AD cases that were predicted (54) and CN cases that were predicted (68), the number of misclassifications was minimal at 4 AD misclassifications and 2 CN misclassifications. The model provides a high degree of confidence that there is good separation between the two subject groups. Finally, Figure 3(d) demonstrates the overall classification of AD with FTD versus CN subjects. The model predicted 54 dementia cases, including AD and FTD, with few misclassifications and strong performance.

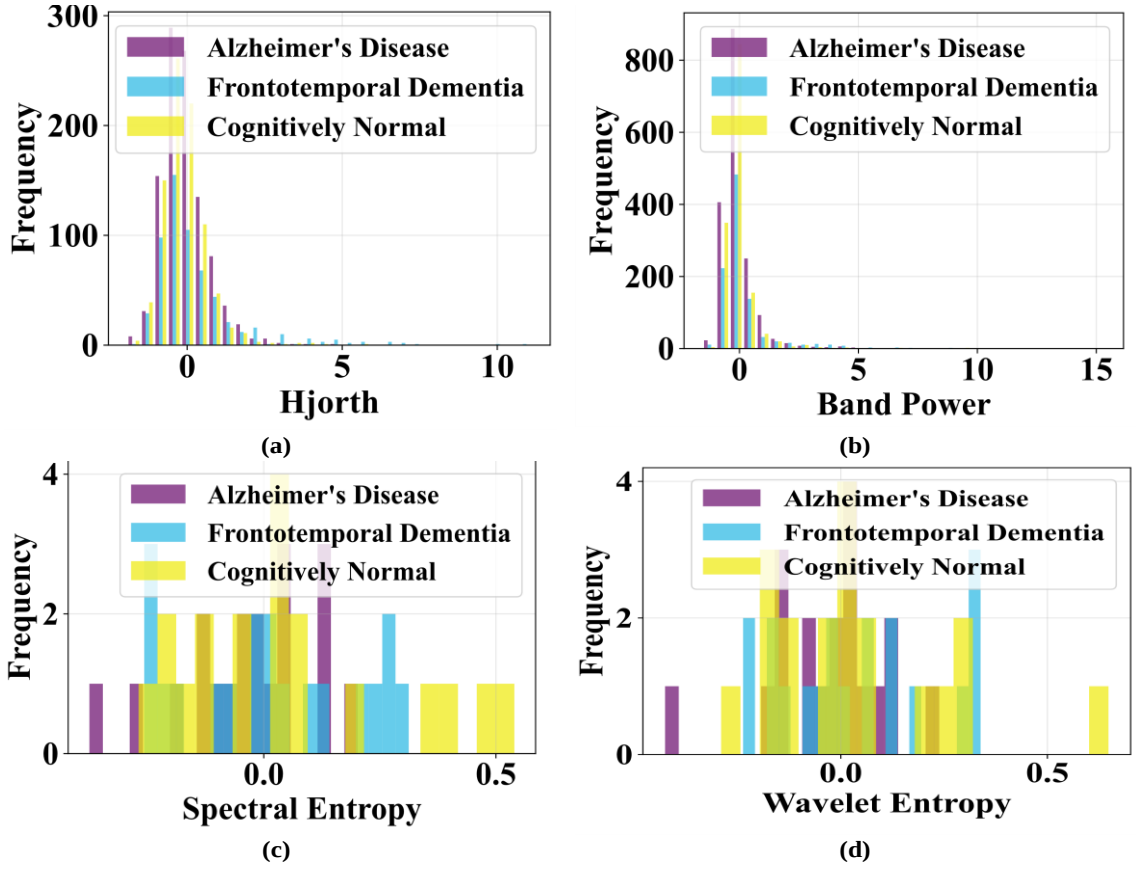

Figure 4: Comparative distribution of Hjorth parameters, Band Power features, Spectral Entropy, and Wavelet Entropy across Alzheimer's Disease (AD), Frontotemporal Dementia (FTD), and Cognitively Normal (CN) groups.

Figure 4 shows the Hjorth variations between control and dementia AD and FTD groups by displaying different levels of temporal activity and reduced complexity within dementia samples. The band power distribution indicates spectral slowing in the AD and FTD clusters that have nearly all the energy within the lower frequency range. Spectral and Wavelet entropy plots demonstrate further differences by indicating decreased signal irregularity and multi-scale complexity for dementia patients compared to CN, who demonstrate a wider range and higher entropy distribution within the same series. Overall, these alternative representations suggest that features that are based on time-domain, frequency-domain, and entropy-based representations effectively capture differences between neurophysiological characteristics resulting from neurodegeneration versus normal brain function.

Table 2: Performance Comparison of Classifiers for AD/FTD/CN Classification

Reference	Classifier	Accuracy	Precision	Recall	F1	Specificity	MCC	AUC	NPV
proposed	SVM-RBF	92.1%	91.7%	92.4%	91.9%	91.6%	87.2%	95.6%	92.3%
Ge et al. [36]	LDA (shrinkage)	88.5%	87.8%	88.1%	87.7%	88.7%	82.5%	92.8%	88.9%
Ahmed et al. [37]	CatBoost	91.3%	90.7%	91.5%	91.0%	91.1%	86.1%	95.0%	91.8%
Kong et al. [38]	LightGBM	90.9%	90.4%	90.8%	90.5%	90.7%	85.6%	94.8%	91.2%
Yi et al. [39]	XGBoost	91.6%	91.1%	91.8%	91.4%	91.2%	86.7%	95.2%	92.0%

Table 3: Performance Comparison of Classifiers for FTD vs CN Classification

Reference	Classifier	Accuracy	Precision	Recall	F1	Specificity	MCC	AUC	NPV
proposed	SVM-RBF	97.9%	97.6%	98.2%	97.8%	97.5%	95.8%	99.2%	97.7%
Ge et al. [36]	LDA (shrinkage)	93.6%	93.2%	94.0%	93.5%	93.0%	87.2%	96.2%	93.4%
Ahmed et al. [37]	CatBoost	96.7%	96.4%	97.1%	96.7%	96.3%	93.5%	98.4%	96.6%
Kong et al. [38]	LightGBM	96.2%	95.8%	96.6%	96.2%	95.6%	92.4%	97.9%	96.1%
Yi et al. [39]	XGBoost	97.1%	96.8%	97.4%	97.1%	96.7%	94.1%	98.6%	96.9%

Table 2 presents the performance comparison of different classifiers for AD/FTD/CN classification. SVM-RBF has the highest total accuracy of 92.1% and AUC (95.6%), suggesting a strong ability to discriminate between the three classes. Additionally, it had the lowest FPR and FNR, indicating a well-balanced sensitivity and specificity. The three boosting models (XGBoost, CatBoost, LightGBM) also performed competitively with accuracies over 90% and AUCs that indicate a strong ability to perform multi-class classification reliably. LDA (shrinkage) performed slightly less than the other classifiers but still provided stable accuracies and balanced evaluation metrics. In summary, SVM-RBF provides the most accurate classification, while all three boosting models (XGBoost, CatBoost, LightGBM) yield strong and consistent classification results for detecting AD/FTD/CN.

Table 3 demonstrate the performance of different classifiers for binary classification between FTD and CN subjects. SVM-RBF achieves the highest accuracy, recall, MCC, and AUC, indicating it is a good classifier and has a low false positive/negative rate. Both (XGBoost) and (CatBoost) were also good classifiers they produced high precision and specificity scores similar to and highly competitive with those of SVM-RBF. Model (LightGBM) performed comparably to SVM-RBF with only small reductions in these metrics. (LDA) produced poorer results than the other classifiers however, it still classified well. Overall, these findings demonstrate that all of the advanced classification techniques identified in this work were highly reliable for classifying subjects with FTD versus CN. Classifier SVM-RBF was the best classifier in all regards, producing superior performance to all other classifiers for identifying subjects with FTD from those who are CN.

Table 4 presents the performance evaluation of different classifiers for binary classification between AD and CN subjects. SVM-RBF achieves the highest overall accuracy, F1-score, MCC, and AUC, indicating strong discriminative performance with low false positive and false negative rates. XGBoost and CatBoost were comparable to SVM in terms of overall metrics, with all 3 classifiers achieving (high) precision, recall, and specificity. The performance for LightGBM was still stable and reliable, there were small reductions in all metrics across the different

classifiers. LDA (Shrinkage) performed lower (in comparison to the other classifiers), but still provided useful classification capability. In summary, the current data show that both SVM and boosting-based models are very successful at identifying individuals with Alzheimer's Disease (AD) compared to cognitively normal (CN) individuals.

Table 4: Performance Comparison of Classifiers for AD vs CN Classification

Reference	Classifier	Accuracy	Precision	Recall	F1	Specificity	MCC	AUC	NPV
proposed	SVM-RBF	95.3%	95.0%	95.6%	95.3%	94.8%	90.6%	97.2%	95.1%
Ge et al. [36]	LDA (shrinkage)	91.8%	91.2%	92.4%	91.7%	91.0%	83.6%	94.3%	91.6%
Ahmed et al. [37]	CatBoost	94.6%	94.2%	95.2%	94.6%	94.0%	89.2%	96.8%	94.4%
Kong et al. [38]	LightGBM	94.1%	93.7%	94.8%	94.2%	93.5%	88.3%	96.3%	93.9%
Yi et al. [39]	XGBoost	94.7%	94.5%	95.2%	94.8%	94.2%	89.7%	96.9%	94.6%

Table 5: Performance Comparison of Classifiers for AD +FTD, CN Classification

Reference	Classifier	Accuracy	Precision	Recall	F1	Specificity	MCC	AUC	NPV
proposed	SVM-RBF	96.9%	96.6%	97.2%	96.8%	96.5%	93.7%	98.2%	97.1%
Ge et al. [36]	LDA (shrinkage)	93.7%	93.4%	94.1%	93.6%	93.5%	87.6%	95.4%	94.0%
Ahmed et al. [37]	CatBoost	95.8%	95.5%	96.1%	95.7%	95.5%	91.7%	97.6%	96.0%
Kong et al. [38]	LightGBM	95.2%	94.9%	95.6%	95.2%	95.1%	90.6%	97.2%	95.4%
Yi et al. [39]	XGBoost	95.8%	95.5%	96.3%	95.8%	95.6%	91.9%	97.8%	96.2%

Table 5 shows the performance of multiple classifiers in distinguishing combined AD and FTD patients from CN subjects. The SVM-RBF produced the highest accuracy (96.9%), F1-score (96.8%), MCC (93.7%) and AUC (98.2%), providing excellent overall discriminative capability, along with providing very low false positive (0.035) and false negative (0.028) rates. The XGBoost and CatBoost provided similar levels of performance, achieving high levels of precision, recall and specificity, while the LightGBM produced stable results that are slightly lower than the other models. The LDA (shrinkage) produced lower performance than the other models, and they still provided reliable classification. Overall SVM and the boosting-based models appear to be better suited for distinguishing AD & FTD from CN subjects.

Figure 5 shows a 2D PCA plot of the EEG features extracted. PCA compresses high-dimensional feature space to two principal components (PC1 and PC2) while preserving maximum variance. The scatter plot indicates clustering tendencies among AD, FTD, and CN groups. CN form a relatively compact cluster AD and FTD samples partially overlap but can be distinguished in specific regions of the feature space. This distribution pattern proves the combined time domain, frequency-domain, and entropy features provide meaningful class separability. This dimensionality reduction analysis also supports downstream ML classifications by validating that the extracted features can catch patterns that are different enough to tell neurodegenerative conditions separately from normal controls.

Figure 6 ROC curve shows the true positive rate varies with the false positive rate of the classifier across various thresholds. Curves nearer the top-left corner indicate that the classifier performs well with respect to distinguishing classes. The AUC for each of the groups is also very high, with AD, FTD, and CN having AUC values of 0.956, 0.949, and 0.951, respectively, which indicates that the model can accurately discriminate between neurodegenerative diseases and subjects that are cognitively normal.

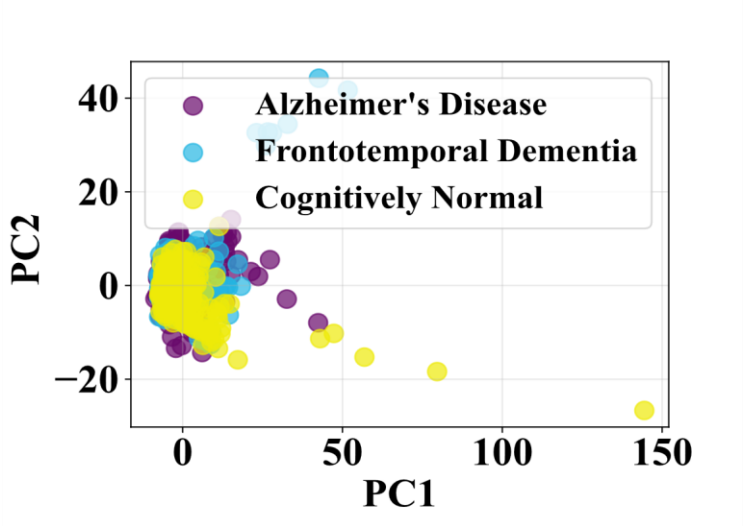

Figure 5: PCA-Based 2D Feature Space Visualization

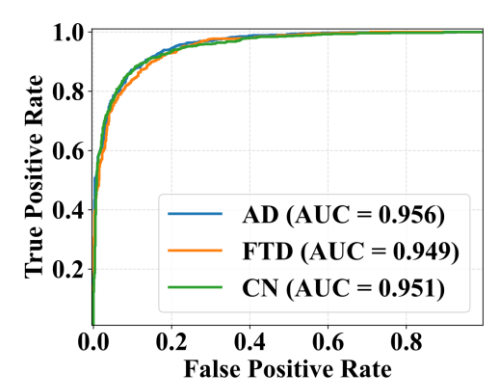

Figure 6: ROC curve of the proposed EEG-based classification model for AD, FTD, and CN detection.

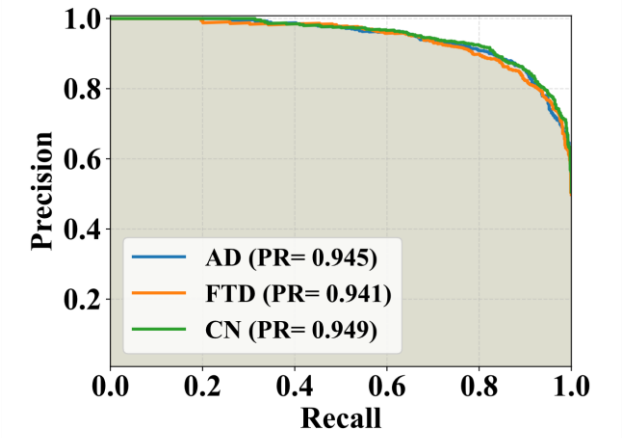

Figure 7: Precision-Recall (PR) curve analysis for the proposed EEG-based classification model across AD, FTD, and CN groups.

Figure 7 shows the precision and recall relate to each other for different classification thresholds. This provides an excellent means of assessing classifier performance when there is class imbalance. The curves are always near the top-right area, meaning high precision at even higher recall levels. The values for the area under the PR curves for

AD, FTD, and CN are AD = 0.945, FTD = 0.941, and CN = 0.949, respectively, indicating that the classifier provides a very strong level of positive predictive power for all of the conditions. The CN class has the highest value on the PR curve, however, both AD and FTD classes also exhibit consistently and reliably high levels of success in accurately identifying neurodegenerative. Overall, this indicates that the specified feature extraction and classification framework can attain a proper balance between sensitivity and precision, with an emphasis on minimizing false positives, while maintaining a high degree of detection for neurodegenerative disease.

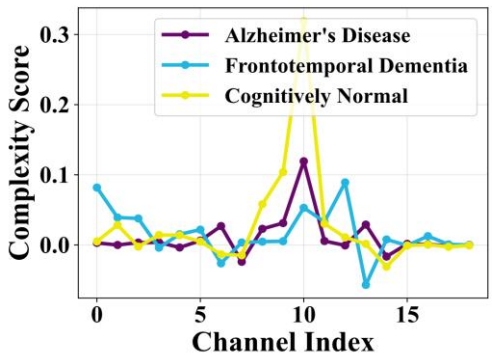

Figure 8: Entropy Complexity Score across EEG channels for Alzheimer's Disease (AD), Frontotemporal Dementia (FTD), and Cognitively Normal (CN) groups.

Figure 8 shows the Entropy Complexity Score is calculate between spectral and wavelet entropies as an overall complexity biological marker. This plot shows that there are differences in the complexity of neural signals by channel across the three groups. CN have on average larger peak values across some channel indices, indicating the neural adaptability of these individuals is not compromised. The AD and FTD groups show lower complexity and less variation in their cortical signal characteristics compared to Controls thus, it appears that People with AD and FTD will have more similar cortical neural signal variabilities than those without the diagnosis of neurodegenerative disease. In general, composite score for entropy also provides an increase in ability to accurately identify developing neurodegeneration.

Figure 9 shows the relationship of the EEG channels through their pairwise correlation coefficients, with values range from -1(solid negative correlation) to +1 (solid positive correlation), where the solid diagonal line is the perfect self-correlation of each channel. The majority of the off-diagonal values show moderate to strong positive correlations, indicating that there is synchrony of neural activity across the frontal Fp1, Fp2, F3, F4, central C3, C4, parietal P3, P4, and occipital O1, O2 regions of interest. The generally stronger correlations between adjacent channel pairs suggest functional connections within the localized cortical network. Thus, the data show interregional synchrony of neural activity, which is important for understanding changes in connectivity in patients with neurodegenerative diseases.

Figure 10 shows the normalized activity in five brain regions frontal, temporal, central, and parietal and occipital. Warm colours denote higher than average activity, and cool colours show reduced activity. This indicates notable regionally redistributed patterns among dementia group have differently coordinated frontal and temporal activity, compared to CN who have significantly symmetrical patterns of activity within the regions. Finally, this figure provides evidence of functional differences between regions of the cortex associated with neurodegenerative disease related to localized cortically altered patterns of functioning.

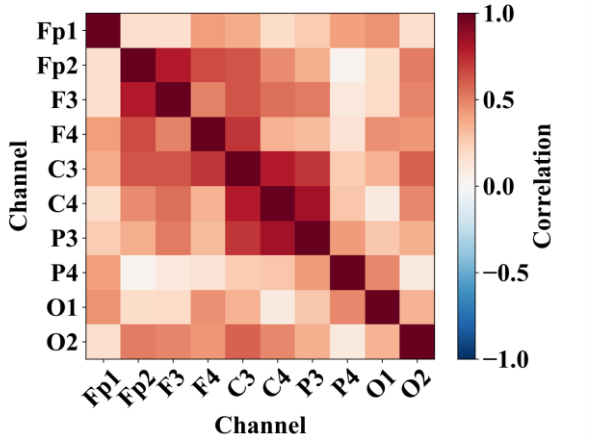

Figure 9: EEG Channel Correlation Heatmap across cortical regions.

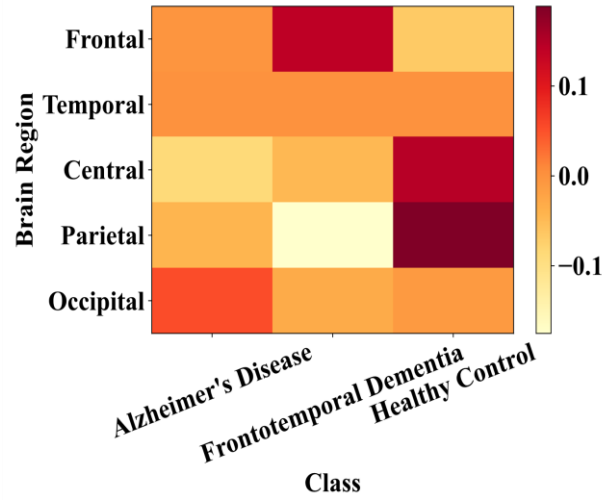

Figure 10: Regional Brain Activity Heatmap across AD, FTD, and CN groups

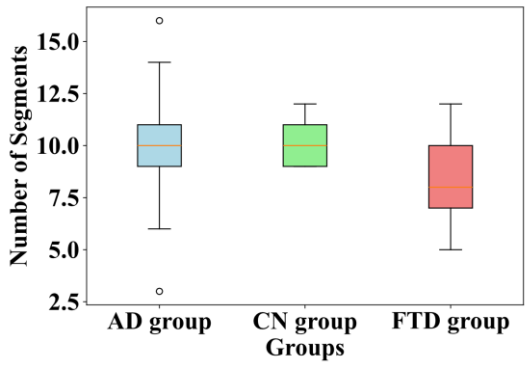

Figure 11: Segment Distribution across AD, CN, and FTD groups.

Figure 11 shows the number of EEG segments extracted per subject within each group. The median line inside each box indicates the central tendency, The Interquartile range (IQR) shows the amount of variability between each sample. The CN exhibits a somewhat normal distribution of segment number since all subjects had relatively equal amounts of segments on average, AD had somewhat greater variability in segment number and had several outliers, indicating that the computer locations and overall segmentation process used to derive the EEG Segments differed

among the subjects. The FTD exhibits the lowest median segment count in comparison to both other groups. Finally, all three groups have relatively similar segment distributions, although there is some variability between segments collected from different subjects, which suggests that fair processes were used in order to prepare the dataset to be classified.

4.2 Ablation Study

Table 6 presents the ablation study for different feature sets contribution to the proposed framework on EEG-based neurodegenerative disease classification. Hjorth time-domain features achieves an accuracy of 80.2% with an AUC of 86.1%, which means that it has moderate discriminative capability but is not very robust. Frequency-domain features improve performance to 87.4% accuracy and 92.4% AUC, indicating that spectral characteristics can provide stronger pathological differentiation than time-domain features. The combination of these two domains increases accuracy to 90.1%, while also raising MCC to 83.4%, thus proving the advantage of multi-domain feature fusion. Finally, in this work, the proposed, time, frequency, and wavelet entropy features together for achieving best performance with 92.1% accuracy and a very high AUC at 95.6%. It also has achieved lowest FPR (0.082) and FNR (0.074). The increasing trend through models clearly shows that adding entropy-based complexity measures significantly improves classification robustness and general diagnostic reliability.

Table 6: Ablation Study on the Effect of Model Components for Suspicious Activity Detection

Feature Set	Accuracy	Precision	Recall	F1-score	Specificity	MCC	AUC	NPV
Hjorth Only	80.2%	79.5%	80.1%	79.8%	81.2%	70.1%	86.1%	80.7%
Frequency Only	87.4%	86.8%	87.9%	86.9%	88.5%	79.2%	92.4%	88.2%
Time + Frequency	90.1%	89.5%	90.8%	89.7%	90.8%	83.4%	94.3%	90.5%
Time + Frequency + Wavelet Entropy	**92.1%**	**91.7%**	**92.4%**	**91.9%**	**91.6 %**	**87.2%**	**95.6%**	**92.3%**

5. Discussion

The proposed hybrid time frequency entropy framework using EEG for the multi-class differentiation between AD, FTD and CN patients shows that integrating time-domain, frequency-domain, and nonlinear entropy-based features significantly enhances diagnostic discrimination compared to single-domain approaches. The proposed SVM-RBF model achieved an overall accuracy of 92.1% and an AUC of 95.6% in multi-class classification, indicating strong separability among the three groups. A key observation from the ablation study is the progressive improvement in classification performance as additional feature domains are incorporated. Using only the Hjorth parameters provide moderate performance with 80.2% accuracy, which shows that time-domain signal variance and slope descriptors are not enough for reliable differentiation of dementia. Once frequency-domain band power features were included, there was a significant improvement to 87.4% accuracy, confirming that spectral slowing and frequency redistribution are critical electrophysiological biomarkers in dementia. The time and frequency combined model further improved classification robustness at 90.1%, which proves the complementary nature of temporal and spectral information.

The highest performance was achieved with the inclusion of Wavelet Entropy resulting in the best performing feature set with an accuracy of 92.1% while also decreasing both FPR and FNR. This clearly includes that nonlinear time-frequency based method, provide significant additional discriminatory information compared to traditional spectral metrics. By comparing the relative changes in entropy features versus traditional spectral metrics, the study demonstrates that reductions in neural dynamical complexity associated with neurodegeneration are effectively captured by entropy features. These findings support previous neurophysiological research suggesting that dementia is characterized by reduced irregularity and adaptability of neural signal processing. The confusion matrix further validates the robustness of the framework, demonstrating that the classifications of all three groups were performed accurately with very little misclassification occurring between AD and FTD classifications. Some degree of overlap was expected due to the commonality of underlying pathological processes and cognitive decline throughout the early stage of this disease. However, the high specificity and MCC values indicate that the classifier provides comparable sensitivity and maintains stable performance even in the presence of class imbalance.

The ROC and Precision-Recall curve analyses further support the robustness of the model. The ROC curves are positioned directly near the upper left area and the respective AUC values AD = 0.956, FTD = 0.949, CN = 0.951, indicate outstanding threshold-independent discriminatory power. This demonstrate that the model maintains high level of precision even at high rates of recall, which is critical in medical diagnostics as it reduces both false positive and false negative. The PCA based visualization supports the quantitative findings by showing clear clustering among the three subject groups in a lower dimensional space. The CN participants formed clusters relatively compact, while the AD and FTD groups show partial but distinct separations. This indicates that the extracted multi-domain features successfully encoded disease-specific neural activity while maintaining class separability. From a neurophysiological perspective, the observed frequency power redistribution and reduced complexity provide meaningful interpretability information for the model. Increased delta and theta power combined with reduced alpha and beta power confirms the well-known phenomenon of EEG slowing in dementia. Additionally, the lower spectral and wavelet entropy values observed in the AD and FTD groups indicate decreased cortical complexity and decreased synaptic dynamics during neurodegeneration. Thus, the composite entropy complexity score strengthens the biomarker by combining irregularity measures on both global and localized levels.

Another advantage of the proposed framework over various ML and DL systems demonstrates its ability to yield high accuracy using hand-crafted and easily interpretable features even with a limited number of patients. The transparency is valuable for clinicians who require understandable models when working with relatively small datasets, which is often the case in proof-of-concepts clinical studies. Z-score normalization was essential to ensure that no single feature dominates the model and to maintain numerical stability during training. Despite the strong performance of the proposed framework, certain limitations remain. The analysis was performed on a moderately sized dataset consist of 88 subjects. Although segmentation increases the number of training samples, clinically valid subgroup cannot be fully established. Future studies should include larger datasets with more than 250 subjects, preferably collected from multi-center cohorts with longitudinal EEG recordings, to better evaluate disease progression. Additional features such as functional connectivity measures or graph-based network metrics may further improve differentiation between AD and FTD. Overall, the results suggest that temporal rhythm characteristics, frequency power redistribution, and nonlinear entropy-based complexity collectively form a comprehensive electrophysiological signature for reliable dementia classification. hybrid time frequency entropy framework using EEG for the multi-class differentiation between AD, FTD and CN patients shows that integrating time-domain, frequency-domain, and nonlinear entropy-based features significantly enhances diagnostic discrimination compared to single-domain approaches. The proposed SVM-RBF model achieved an overall accuracy of 92.1% and an AUC of 95.6% in multi-class classification, indicating strong separability among the three groups. A key observation from the ablation study is the progressive improvement in classification performance as additional feature domains are incorporated. Using only the Hjorth parameters provide moderate performance with 80.2% accuracy, which shows that time-domain signal variance and slope descriptors are not enough for reliable differentiation of dementia. Once frequency-domain band power features were included, there was a significant improvement to 87.4% accuracy, confirming that spectral slowing and frequency redistribution are critical electrophysiological biomarkers in dementia. The time and frequency combined model further improved classification robustness at 90.1%, which proves the complementary nature of temporal and spectral information.

The highest performance was achieved with the inclusion of Wavelet Entropy resulting in the best performing feature set with an accuracy of 92.1% while also decreasing both FPR and FNR. This clearly includes that nonlinear time-frequency based method, provide significant additional discriminatory information compared to traditional spectral metrics. By comparing the relative changes in entropy features versus traditional spectral metrics, the study demonstrates that reductions in neural dynamical complexity associated with neurodegeneration are effectively captured by entropy features. These findings support previous neurophysiological research suggesting that dementia is characterized by reduced irregularity and adaptability of neural signal processing. The confusion matrix further validates the robustness of the framework, demonstrating that the classifications of all three groups were performed accurately with very little misclassification occurring between AD and FTD classifications. Some degree of overlap was expected due to the commonality of underlying pathological processes and cognitive decline throughout the early stage of this disease. However, the high specificity and MCC values indicate that the classifier provides comparable sensitivity and maintains stable performance even in the presence of class imbalance.

The ROC and Precision-Recall curve analyses further support the robustness of the model. The ROC curves are positioned directly near the upper left area and the respective AUC values AD = 0.956, FTD = 0.949, CN = 0.951, indicate outstanding threshold-independent discriminatory power. This demonstrate that the model maintains high level of precision even at high rates of recall, which is critical in medical diagnostics as it reduces both false positive

and false negative. The PCA based visualization supports the quantitative findings by showing clear clustering among the three subject groups in a lower dimensional space. The CN participants formed clusters relatively compact, while the AD and FTD groups show partial but distinct separations. This indicates that the extracted multi-domain features successfully encoded disease-specific neural activity while maintaining class separability. From a neurophysiological perspective, the observed frequency power redistribution and reduced complexity provide meaningful interpretability information for the model. Increased delta and theta power combined with reduced alpha and beta power confirms the well-known phenomenon of EEG slowing in dementia. Additionally, the lower spectral and wavelet entropy values observed in the AD and FTD groups indicate decreased cortical complexity and decreased synaptic dynamics during neurodegeneration. Thus, the composite entropy complexity score strengthens the biomarker by combining irregularity measures on both global and localized levels.

Another advantage of the proposed framework over various ML and DL systems demonstrates its ability to yield high accuracy using hand-crafted and easily interpretable features even with a limited number of patients. The transparency is valuable for clinicians who require understandable models when working with relatively small datasets, which is often the case in proof-of-concepts clinical studies. Z-score normalization was essential to ensure that no single feature dominates the model and to maintain numerical stability during training. Despite the strong performance of the proposed framework, certain limitations remain. The analysis was performed on a moderately sized dataset consist of 88 subjects. Although segmentation increases the number of training samples, clinically valid subgroup cannot be fully established. Future studies should include larger datasets with more than 250 subjects, preferably collected from multi-center cohorts with longitudinal EEG recordings, to better evaluate disease progression. Additional features such as functional connectivity measures or graph-based network metrics may further improve differentiation between AD and FTD. Overall, the results suggest that temporal rhythm characteristics, frequency power redistribution, and nonlinear entropy-based complexity collectively form a comprehensive electrophysiological signature for reliable dementia classification.

6. Conclusion

This study presented the hybrid approach to improve the accuracy of diagnosis for AD, FTD and CN populations by developing an EEG and multiple domains classification system. The new hybrid classification system utilized four groups of features Hjorth parameters, band power analysis, spectral entropy, and wavelet entropy that were combined with a RBF classifier. The results showed high diagnostic performance with an AUC of 95.6% and an overall accuracy rate of 92.1%. The results of the ablation study indicate that the integration of multiple feature domains, using entropy type complexity measures, supporting significantly to the robustness and reliability of classification output. The framework shows evidence of capturing neurodegeneration-related changes associated with spectral slowing, irregularities, and reduced cortical complexity. The proposed method offers an efficient, interpretable, and clinically scalable method for the early identification of dementia in patients. Future work will include expanding the dataset, applying connectivity-based biomarker analysis, and exploring longitudinally predictive modelling to improve the clinical applicability of the hybrid model.

Statements and Declarations

Author contributions: All authors contributed to the conception of the problem setting and overall design of the work. P. G built the conceptualization and methodology. J. S implemented the work, and writing. Authors, involved into visualization of concepts. This version was revised and improved by all authors, who also read and approved the final manuscript.

Funding: No funding was received to conduct this study.

Conflict of interest: The authors declare no conflict of interest.

Availability of data and materials:

https://figshare.com/articles/dataset/fMRI_data/14675505/1?file=28177734

Ethical approval: The research is original and all the figures and tables are created by the authors of this manuscript.

Consent to participate: Not applicable.

Consent for publication: All authors agree with the submission of the manuscript to this journal and possible publication afterwards.

References

1. M. Acharya, R. C. Deo, X. Tao, P. D. Barua, A. Devi, A. Atmakuru, R. S. Tan. "Deep learning techniques for automated Alzheimer's and mild cognitive impairment disease using EEG signals: A comprehensive review of the last decade (2013-2024)", Computer Methods and Programs in Biomedicine, 259 (1), pp. 108506, 2025.
2. F. Akbar, I. Taj, S. M. Usman, A. S. Imran, S. Khalid, I. Ihsan, A. Ali, A. Yasin. "Unlocking the potential of EEG in Alzheimer's disease research: Current status and pathways to precision detection", Brain Research Bulletin, 223 (2), 111281, 2025.
3. K. Rezaee, M. Zhu. "Diagnose Alzheimer's disease and mild cognitive impairment using deep CascadeNet and handcrafted features from EEG signals", Biomedical Signal Processing and Control, 99 (3), 106895, 2025.
4. D. V. Puri, J. P. Gawande, P. H. Kachare, I. Al-Shourbaji. "Optimal time-frequency localized wavelet filters for identification of Alzheimer's disease from EEG signals", Cognitive Neurodynamics, 19 (1), 12, 2025.
5. S. Jain, R. Srivastava. "Enhanced EEG-based Alzheimer's disease detection using synchrosqueezing transform and deep transfer learning", Neuroscience, 576, 105-117, 2025.
6. M. Rostamikia, Y. Sarbaz, S. Makouei. "EEG-based classification of Alzheimer's disease and frontotemporal dementia: a comprehensive analysis of discriminative features", Cognitive Neurodynamics, 18 (6), 3447-3462, 2024.
7. J. Cao, B. Li, X. Li. "Identification of Alzheimer's disease brain networks based on EEG phase synchronization", Biomedical engineering online, 24 (1), 32, 2025.
8. Y. Liu, L. An, H. Yang, S. S. Ge. "Multi-frequency EEG and multi-functional connectivity graph convolutional network based detection method of patients with Alzheimer's disease", Complex & Intelligent Systems, 11 (8), 366, 2025.
9. K. Ghassemkhani, K. S. Saroka, B. T. Dotta. "Evaluating EEG complexity and spectral signatures in Alzheimer's disease and frontotemporal dementia: evidence for rostrocaudal asymmetry", npj Aging, 11 (1), 50, 2025.
10. I. Sercek, N. Sampathila, I. Tasci, T. Ekmekyapar, B. Tasci, P. D. Barua, M. Baygin, S. Dogan, T. Tuncer, R.S. Tan, U. R. Acharya. "A new quantum-inspired pattern based on Goldner-Harary graph for automated alzheimer's disease detection", Cognitive Neurodynamics, 19 (1), 71, 2025.
11. S. Schwerin, S. Z. Dragovic, J. Ostertag, D. M. Nguyen, G. Schneider, M. Kreuzer. "EEG features associated with Alzheimer's disease and Frontotemporal dementia are not reflected by processed indices used in anesthesia monitoring", Journal of Clinical Monitoring and Computing, 39 (4), 681-696, 2025.
12. S. Siuly, M. N. A. Tawhid, Y. Li, R. Acharya, M. T. Sadiq, H. Wang. "Investigating brain lobe biomarkers to enhance dementia detection using EEG data", Cognitive Computation, 17 (2), 90, 2025.
13. W. Qi, X. Zhu, B. Wang, Y. Shi, C. Dong, S. Shen, J. Li, K. Zhang, Y. He, M. Zhao, S. Cao. "Alzheimer's disease digital biomarkers multidimensional landscape and AI model scoping review", npj Digital Medicine, 8 (1), 366, 2025.
14. R. Wang, H. Xu, D. Yi, C. Song, Y. Che. "Automatic detection of Alzheimer's disease from EEG signals using hybrid PSO-GWO algorithm", Biomedical Signal Processing and Control, 107 (4), 107798, 2025.
15. K. I. Jang, Y. I. Kim, H. J. Ju, S. J. An, P. W. Park. "Dementia classification using two-channel electroencephalography features", Scientific Reports, 15 (1), 11513, 2025.
16. G. Zamboni, R. Maramotti, S. Salemme, M. Tondelli, G. Adani, G. Vinceti, C. Carbone, T. Filippini, M. Vinceti, G. Pagnoni, A. Chiari. "Age-specific prevalence of the different clinical presentations of AD and FTD in young-onset dementia", Journal of neurology, 271 (7), 4326-4335, 2024.
17. S. K. Lakshmanan, M. Muthusamy, R. K. Dhanaraj, A. Sureshkumar, M. S. Sayeed, M. Y. N. Mohamed, G. Rathinam. "Effective deep convolutional neural network with attention mechanism for Alzheimer disease classification," Frontiers in Radiology, 5 (5), 1698760, 2025.
18. A. G. D. J. Raju, S. S. Manohar, T. C. J. Jeaunita. "Mitigating catastrophic forgetting in imitation learning for embodied AI using progressive neural networks", Econom. Comput. Econom. Cybernet. Stud. Res., 59(3), 97-112, 2025.
19. M. Le Acharya, R. C. Deo, P. D. Barua, A. Devi, X. Tao. "EEGConvNeXt: a novel convolutional neural network model for automated detection of Alzheimer's disease and frontotemporal dementia using EEG signals", Computer Methods and Programs in Biomedicine, 262 (3), 108652, 2025.
20. F. Akbar, Y. Alkhrijah, S. M. Usman, S. Khalid, I. Ihsan, M. A. Alawad. "NeuroFusionNet: a hybrid EEG feature fusion framework for accurate and explainable Alzheimer's Disease detection", Scientific Reports, 15 (1), 43742, 2025.
21. H. S. Ohal, S. Mantri. "Exploring EEG-based biomarkers for improved early Alzheimer's disease detection: a feature-based approach utilizing machine learning", Measurement: Sensors, 36 (3), 101403. 2024.
22. S. Abadal, P. Galván, A. Mármol, N. Mammone, C. Ieracitano, M. L. Giudice, A. Salvini, F. C. Morabito. "Graph neural networks for electroencephalogram analysis: Alzheimer's disease and epilepsy use cases", Neural Networks, 181(2), 106792, 2025.
23. Y. Si, R. He, L. Jiang, D. Yao, H. Zhang, P. Xu, X. Ma, L. Yu, F. Li. "Differentiating between Alzheimer's disease and frontotemporal dementia based on the resting-state multilayer EEG network", IEEE Transactions on Neural Systems and Rehabilitation Engineering, 31(2), 4521-4527, 2023.
24. D. V. Puri, P. H. Kachare, S. B. Sangle, R. Kirner, A. Jabbari, I. Al-Shourbaji, M. Abdalraheem, A. Alameen. "Leadnet: detection of alzheimer's disease using spatiotemporal eeg analysis and low-complexity cnn", IEEE Access, 12 (4), 113888-113897, 2024.
25. https://github.com/OpenNeuroDatasets/ds004504

26. M. N. A. Tawhid, S. Siuly, E. Kabir, Y. Li. “Advancing Alzheimer’s disease detection: a novel convolutional neural network-based framework leveraging EEG data and segment length analysis: MN Ahad Tawhid et al.”, Brain Informatics, 12 (1), 13, 2025.
27. J. Zhang, T. Tan, Y. Jiang, C. Tan, L. Hu, D. Xiong, Y. Ding, G. Huang, J. Qin, Y. Tian. “Working-memory load decoding model inspired by brain cognition based on cross-frequency coupling”, Brain Research Bulletin, 221 (2), 111206, 2025.
28. R. Al Hasan, M. H. Saberi, M. A. Riahi, “Seismic facies classification and TOC prediction using seismic attributes and Hjorth parameters, in the Groningen field in northeastern Netherlands”, Discover Applied Sciences, 7 (10), 1202, 2025.
29. T. Devanand, C. S. A. Sekhar, T. Aktürk, I. Kiyi, G. Yener, B. Güntekin, J. Joseph, C. Adaikkan. “EEG biomarkers in Alzheimer’s and prodromal Alzheimer’s: A comprehensive analysis of spectral and connectivity features”, Alzheimer’s research & therapy, 16 (1), 236, 2024.
30. B. R. Nayana, M. N. Pavithra, S. Chaitra, T. N. Bhuvana Mohini, T. Stephan, V. Mohan, N. Agarwal. “EEG-based neurodegenerative disease diagnosis: comparative analysis of conventional methods and deep learning models,” Scientific Reports, 15 (1), 15950, 2025.
31. U. Aslan, M. F. Akşahin. “Detection of alzheimer and mild cognitive impairment patients by poincare and entropy methods based on electroencephalography signals”, BioMedical Engineering OnLine, 24 (1), 47, 2025.
32. Z. Liu, B. Zhu, M. Hu, Z. Deng, J. Zhang. “Revised tunable Q-factor wavelet transform for EEG-based epileptic seizure detection”, IEEE Transactions on Neural Systems and Rehabilitation Engineering, 31, 1707-1720, 2023.
33. N. H. Kim, U. Park, D. W. Yang, S. H. Choi, Y. C. Youn, S. W. Kang. “PET-validated EEG-machine learning algorithm predicts brain amyloid pathology in pre-dementia Alzheimer’s disease”, Scientific Reports, 13 (1), 10299, 2023.
34. M. Vishwanath, S. Cao, N. Dutt, A. M. Rahmani, M. M. Lim, H. Cao, “Reducing interdataset covariate shift in sleep EEG of traumatic brain injured humans and mice using Transfer Euclidean Alignment”, Biomedical Signal Processing and Control, 108 (2), 107948, 2025.
35. M. D. Rajab, E. Jammeh, T. Taketa, C. Brayne, F. E. Matthews, L. Su, P.G. Ince, S.B. Wharton, D. Wang, Cognitive Function and Ageing Neuropathology Study Group. “Assessment of Alzheimer-related pathologies of dementia using machine learning feature selection”, Alzheimer's Research & Therapy, 15 (1), 47, 2023.
36. Y. Ge, J. Yin, C. Chen, S. Yang, Y. Han, C. Ding, J. Zheng, Y. Zheng, J. Zhang, “An EEG-based framework for automated discrimination of conversion to Alzheimer’s disease in patients with amnestic mild cognitive impairment: an 18-month longitudinal study”, Frontiers in Aging Neuroscience, 16 (3), 1470836, 2025.
37. M. A. O. Ahmed, Y. A. Satar, E. M. Darwish, E. A. Zanaty, “Synergistic integration of Multi-View Brain Networks and advanced machine learning techniques for auditory disorders diagnostics’, Brain Informatics, 11 (1), 3, 2024.
38. J. Kong, M. So, H. Park, Y. T. Kim, H. Kim, K. Pahk, S.H. Kang, S. Do, D.K. Lim, C.N. Lee, J. B. Kim. “Electroencephalography functional network for screening amyloid positivity in mild cognitive impairment: a cross-sectional study”, Clinical Neurophysiology, 180 (2), 2111374, 2025.
39. F. Yi, H. Yang, D. Chen, Y. Qin, H. Han, J. Cui, W. Bai, Y. Ma, R. Zhang, H. Yu, “XGBoost-SHAP-based interpretable diagnostic framework for alzheimer’s disease”, BMC medical informatics and decision making, 23 (1), 137, 2023.